

STRUCTURE AND PROPERTIES OF THE DEFORMED STATE

Effect of Severe Plastic Deformation on the Acoustic Emission and the Thermal Effects in Titanium Nickelide

N. N. Belousov^{a, †}, V. A. Andreev^{b, c}, E. V. Chernyaeva^{d, *}, A. E. Volkov^d, and Yu. N. V'yunenko^e

^aGalkin Donetsk Institute for Physics and Technology, Donetsk, 83114 Ukraine

^bOOO Matek-Sma Industrial Center, Moscow, 117449 Russia

^cBaikov Institute of Metallurgy and Materials Science, Russian Academy of Sciences, Moscow, 119334 Russia

^dSt. Petersburg State University, St. Petersburg, 198504 Russia

^eOOO Optimikst LTD, St. Petersburg, 195426 Russia

*e-mail: lena@smel.math.spbu.ru

Received December 5, 2018; revised December 13, 2018; accepted December 20, 2018

Abstract—Acoustic emission and differential scanning calorimetry have been used to study the structural changes and the thermal effects in a TiNi alloy after severe plastic deformation (SPD). The character and the thermal effect after SPD are shown to demonstrate partial amorphization of the alloy. The heat release observed upon the first heating after SPD in the temperature range 250–380°C corresponds to solidification. The number of detected acoustic emission signals from the TiNi alloy and their amplitudes are found to decrease after SPD.

Keywords: severe plastic deformation (SPD), torsion under quasi-hydrostatic pressure, acoustic emission, martensitic transformation, shape memory alloy, differential scanning calorimetry

DOI: 10.1134/S0036029519100021

INTRODUCTION

The martensitic transformation in titanium nickelide is accompanied by acoustic radiation generated by the transformation of the crystal lattice [1]. Studies showed the dependence of the acoustic effect on the physicochemical properties of the material, which influences the phase transition; in particular, the characteristic of the acoustic radiation are changed as the chemical composition is changed [2]. Thermal cycling with the transformation of the material from the martensitic state into the austenitic state and vice versa markedly decreases the acoustic emission (AE) intensity [3]. However, its level is restored to a significant degree within 48 h [4].

An increase in the heating rate favors an increase in the energy and number of generated pulses [4], which is likely to be related to the expansion of the zone from which acoustic signals are detected.

In [5], additional AE signals were detected due to the inverse martensitic transformation when it accompanied by the shape recovery. Thus, AE enables one to obtain data on the deformation phenomena that accompany the phase transition.

The studies of the acoustic radiation during indentation of a hard-alloy indenter into samples of tita-

nium nickelide with a gradient structure demonstrate a dependence of AE on the state of the material. Indentation [6] was performed for various regions in disc-like samples fabricated of the Ti–55.15Ni alloy (wt %) by rotational forging [7, 8]. Calorimetric studies showed comparable temperatures A_{on} (63.6–65.7°C) and A_f (83.5–85°C) and comparable latent heat of transformation (24.1–24.5 J/g) in three regions disposed at various distances from the center of a sample. The spectral power densities of the AE signals recorded from these regions during indentations were substantially different.

The AE sensitivity to changes in the structure of the material was used to study the effect of severe (large or megaplastic [9]) plastic deformation (SPD) on the structure of the TiNi alloy and to investigate the thermal characteristics of the martensitic transformations.

EXPERIMENTAL

We studied 2-mm-thick disc-like samples cut from a Ti–55.15Ni (wt %) alloy rod with an electric spark. The rod was fabricated by rotational forging. The rod was forged to diameter of 12 mm at a temperature of 800°C and to diameter of 10 mm at 400°C. According to the calorimetric studies [6], the alloy was in the martensitic state after this treatment. Some discs were deformed at room temperature by torsion in the Bridg-

[†] Deceased.

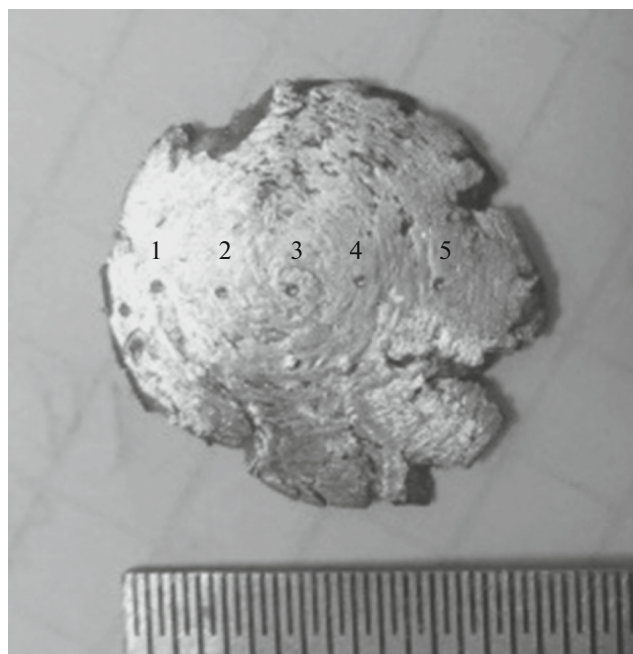


Fig. 1. TiNi alloy sample after SPD; numerals indicate the places of indentations.

man anvils-type setup developed and manufactured at the Donetsk Institute for Physics and Technology [10]; the test conditions were as follows: the load was 2 GPa, the strain rate 5 rpm, and the number of revolutions was 10.

AE was initiated by the indentation of a hard-alloy conical indenter into a sample at a rate of 1.0 mm/min in an IM-4A testing machine. The maximum indentation load was 1000 N. After SPD, indentation was carried out at five points along the sample diameter (Fig. 1). AE signals were detected and converted into electrical signals using an MSAE-L2 broadband AE detector and an MSAE-FA010 amplifier at a total

amplification of 80 dB and a transmission band of 60–1000 kHz. To perform calorimetric studies on a Mettler Toledo 822E differential scanning calorimeter, we cut samples from the zones adjacent to indentations. The calorimetric studies were performed at a heating or cooling rate of 10°C/min.

RESULTS AND DISCUSSION

In the case of indentation of the initial samples, about 280 AE signals were recorded on average. After SPD, the number of AE signals decreased to 212. According to the averaged spectral power density of the AE signals in the region close to the undamaged lateral sample surface (Fig. 1, point 1), the spectral density curve is similar to that for the initial material (Figs. 2a, 2b). This is likely to be related to the cyclicity of structure development at SPD, which leads to the formation of a state close to the initial one [9, 11]. The second maximum in height in these curves is near 250 kHz.

The spectra of the signals obtained for point 2 and 3 have similar frequency characteristics with higher peaks at frequencies 135 and 170 kHz (Figs. 2c, 2d). Point 4 is close to the most damaged region and this fact is observed in the spectral density of the AE power: higher frequencies begin to dominate there (Fig. 2e).

Point 5 is in the sample cracking zone. The AE signals from this zone have very wide spread in parameters, although the averaged curve is similar to curves 2 and 3 but with a clearer maximum at 400–500 kHz (Fig. 2f).

The calorimetric studies were performed in various temperature ranges. Table 1 gives the characteristic temperatures and the specific heat release (heat absorption) at phase transformations. Sample 1 was heated from room temperature to 200°C. According to the obtained data, a weak endothermic reaction with an absorption energy of 1.2 J/g occurs in the tempera-

Table 1. Characteristic temperatures and thermal effects at phase transitions in the TiNi alloy after SPD

Sample	T_{\max} , °C	Heating 1			Cooling			Heating 2		
		A_{s1} , °C	A_{f1} , °C	q , J/g	M_s , °C	M_f , °C	q , J/g	A_{s1} , °C	A_{f1} , °C	q , J/g
1	200	54	135	–1.2	–	–	–	–	–	–
2	300	45	133	–1.1	67	Below –100	N/A	–23	77	–2.5
3	300	46	137	–1.2	71	–100	N/A	–26	70	–3.9
4	400	80	140	–1	62	33.5	19.0	16	64	–14.9
5	400	288	368	9.0	–2	100	19.0	41		
		80	150	–1	63	26.3	20.0	20	65	–15.0
		247	385	20	8	Below –100	20.0	41		

* T_{\max} is the maximum heating temperature; A_{s1} and A_{f1} are the start and finish inverse transformation temperatures on the first heating, respectively; M_s and M_f are the start and finish forward transformation temperatures on cooling after the first heating, respectively; A_{s2} and A_{f2} are the start and finish inverse transformation temperatures on the second heating, respectively; and q is the specific heat release (absorption); and N/A means that the value was not measured.

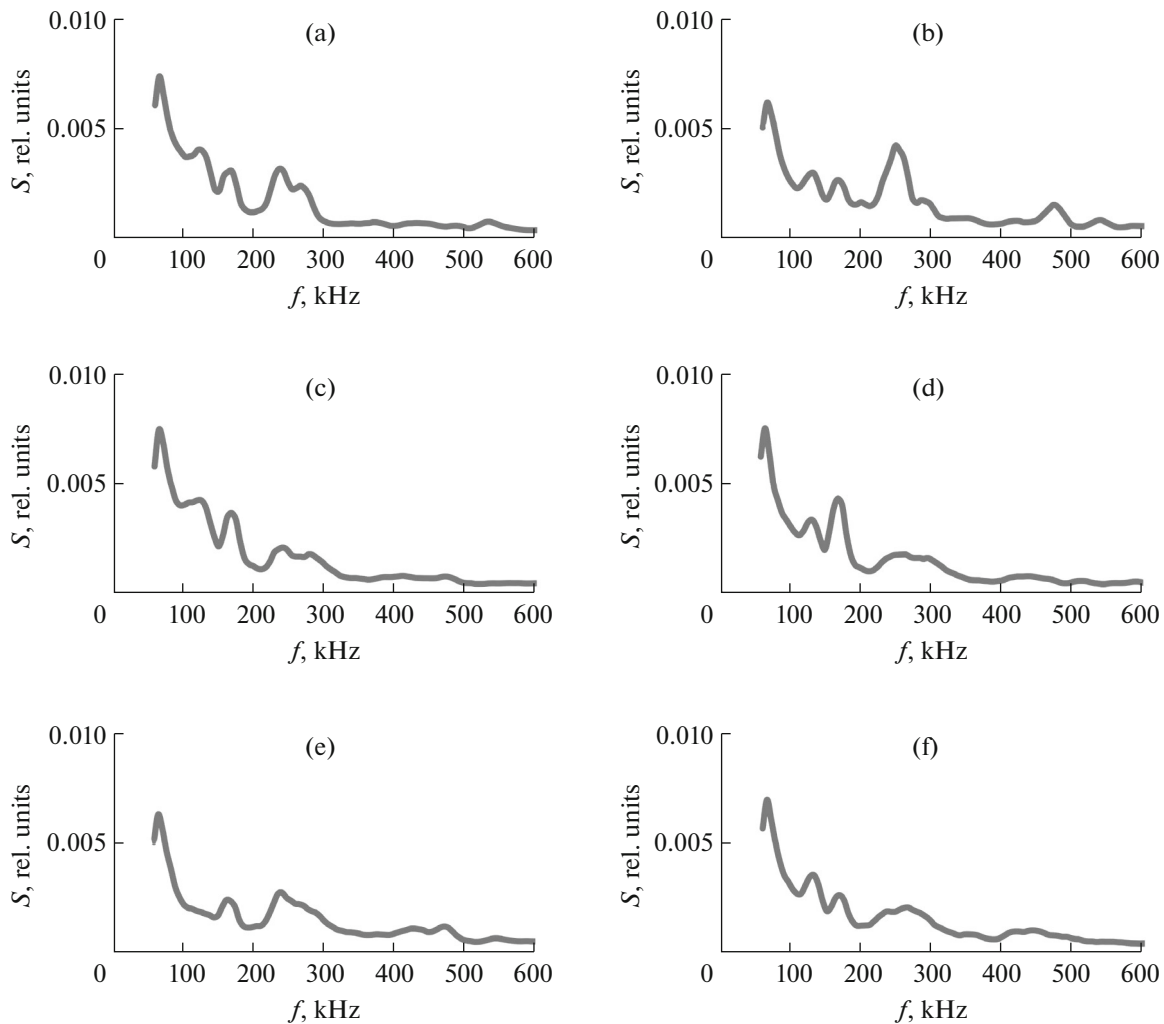


Fig. 2. Spectral power densities of the AE signal detected during indentation into a TiNi alloy sample (a) in the initial state and (b–f) after SPD at points 1–5.

ture range 50–140°C (Fig. 3a). No marks of phase or structural transitions were observed on cooling from 200 to –100°C, as well as on repeated heating to 200°C.

Samples 2 and 3 were heated to 300°C. Their calorimetric curves, as well as the curves of the spectra density of AE signals, are very similar. In the range 50–150°C, both samples demonstrate endothermic processes. The additional heat absorption is 1.1 J/g in sample 2 (Fig. 3b) and 1.2 J/g in sample 3 (Fig. 3c). Further heating to 300°C is not accompanied by endothermic effects. An exothermic process was observed on cooling in the range from 71 to –100°C, and repeated heating is accompanied by heat absorption of 2.5 and 3.9 J/g for samples 2 and 3, respectively.

Sample 4 was heated to 400°C. Near 100°C, we observed a weak endothermic process with a heat accumulation of ~1 J/g (Fig. 3d). Above 280°C, an exothermic process starts and continues to 370°C. In

this case, the exothermic effect is 9 J/g. On cooling from 400°C, two exothermic reactions occur: the first maximum was fixed at 53°C and the second peak, at –45°C. The repeated heating leads to the formation of a double peak in the range 15–65°C. The maximum heat absorption was observed at 58°C.

The calorimetric curves for samples 4 and 5 are qualitatively similar. The exothermic reaction characteristics are different only during the first heating (Fig. 4). For example, the heat release in sample 4 begins at 280°C, its maximum intensity is observed at 342°C, and the end is at 370°C. For sample 5, the corresponding values are 250, 343, and 380°C. The heat release during these reactions is 9 and 20 J/g for samples 4 and 5, respectively.

The data on the amorphization of a titanium–nickel alloy as a result of SPD were presented in [12]. This effect is likely to become determining in changing the characteristics of AE and thermal effects in tita-

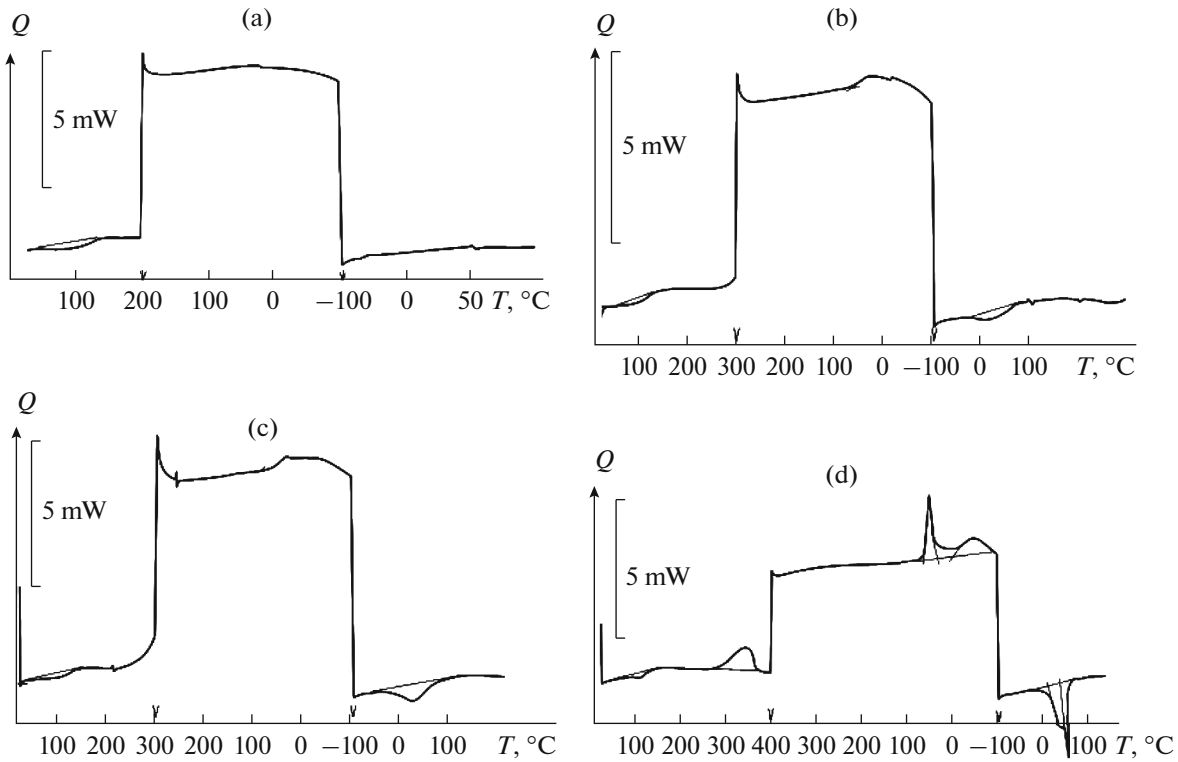


Fig. 3. Calorimetric curves for samples (a) 1, (b) 2, (c) 3, and (d) 4.

nium nickelide studied in this work. A comparison of AE on the indentation of the TiNi alloy samples in the initial state and after SPD demonstrates a decrease in the number of recorded AE signals and a decrease in their amplitudes. A similar effect was also observed in other materials, for example, in aluminum, after equal-channel angular pressing (ECAP) [13]. It was noted in [14] that grain refinement is a factor of

decreasing the acoustic signal amplitude. It seems likely that this is one of the causes of the observed phenomenon. In this case, the spectral curves of AE signals for the strongly deformed material tend to shift to higher frequencies (Figs. 2e, 2f). We do not know similar interpretation of the changes in the AE spectra as a result of SPD for shape memory alloys.

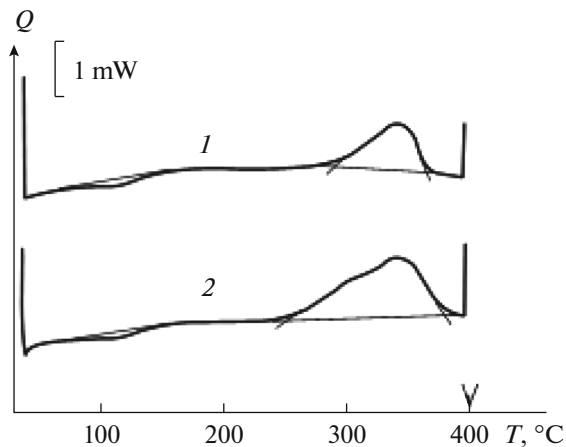


Fig. 4. Calorimetric curves (first heating to 400°C) for samples (1) 4 and (2) 5.

During the first heating after SPD, a weak heat absorption peak is observed in the temperature range 50–150°C, which corresponds to the $B19'$ – $B2$ transition, and a heat release peak is observed in the temperature range 250–380°C (Fig. 4). During the second heating, the heat absorption peak at the martensitic transition is pronounced. We can conclude that the material is partially amorphized upon SPD and crystallizes during the first heating at 250–380°C. However, the obtained data are insufficient to understand the nature of the crystalline phase: whether it is the retained initial martensite or a product of dynamic solidification [9]. Note, that the heat absorption peak during the second heating is in the temperature range 20–65°C; i.e., the transformation takes place at lower temperatures than the temperature immediately after SPD. Thus, we observe the effect of martensite stabilization as a result of a deformation in the martensitic state, which was studied, for example, in [15, 16].

A comparison of the calorimetric curves for the samples underwent incomplete (samples 2 and 3, heating to 300°C) and complete (sample 4, heating to 400°C) crystallization (Figs. 3b–3d) showed that the phase transition after crystallization becomes two-stage: at the first stage, as well as after ECAP [17], the alloy is likely to transform into the rhombohedral phase. The further cooling of the alloy in the range from 0°C to –100°C led to the R – $B19'$ transformation, which was demonstrated by the second peak of the exothermic reaction. In this case, the double peak at repeated heating can demonstrate incomplete R – $B19'$ phase transformation; as a result, the transition to the austenitic state occurs from both martensite $B19'$ and the rhombohedral phase.

An essential moment is the change in the phase transition temperatures at repeated heating. After partial crystallization of samples 2 and 3, the maximum intensity of the endothermic reaction is observed at 27°C, and it is at 57°C after complete transition to the crystalline state of sample 4. In this case, the peak is doubled: the first maximum is at 27°C and the second maximum is at 57°C (Fig. 3d). The heat absorption is likely to be determined by the degree of crystallization, and it is 15 J/g for sample 4 as compared to 2.5 and 3.9 J/g for samples 2 and 3, respectively (Table 1).

It should be noted that the heat release of sample 5 increases by a factor of more than two as compared to that of sample 4 (Table 1, Fig. 4), which can be related to an increase in SPD with the distance from the torsion axis. It is clear that the fraction of an amorphous phase increases with SPD.

CONCLUSIONS

AE during indentation of TiNi alloy samples in the initial state and after SPD demonstrates a decrease in the number of recorded signals and a decrease in their amplitude in the deformed material, which shows that the size of the regions subjected to plastic shears decreases. The calorimetric studies revealed a weak heat absorption peak in the temperature range 50–150°C corresponding to the $B19'$ – $B2$ transition during the first heating and a heat release peak related to crystallization in the temperature range 250–380°C. During the second heating, there are pronounced heat absorption peaks related to the $B19'$ – R and R – $B2$ transformations in the temperature range 20–65°C. Higher temperatures of the inverse martensitic transformation during the first heating demonstrate martensite stabilization.

ACKNOWLEDGMENTS

The authors are grateful to N.N. Resnina for her help in the calorimetric studies.

REFERENCES

1. A. I. Potekaev and V. A. Plotnikov, *Acoustic Dissipation of Energy at Thermoelastic Martensitic Transformations* (NTL, Tomsk, 2004).
2. V. A. Plotnikov, A. S. Gryaznov, and I. V. Kharlamov, “Acoustic emission and deformation at cycling of martensitic transformations of titanium-nickelide-based alloys under mechanical loading,” *Vestn. AltGTA. Estestv. Tochnye Nauki*, No. 13, 18–23 (2012).
3. V. A. Plotnikov, A. A. Kovalenko, D. V. Kokhanenko, and A. D. Nasonov, “Acoustic emission and anomalous behavior of elastic moduli at thermoelastic martensitic transformations,” *UI'trazvuk Termodin. Svoistva Veshch.*, No. 29, 31–34 (2003).
4. Yu. N. V'yunenko and E. V. Chernyaeva, “Effect of conditions of thermocycling of a TiNi alloy on the acoustic emission parameters, in *Proceedings of XXII Petersburg Readings on the Strength Problems* (Poltekh Univer., St. Petersburg, 2016), pp. 387–389.
5. Yu. N. V'yunenko, V. V. Kozhushko, A. E. Volkov, and E. V. Chernyaeva, “Acoustic emission at the thermocycling of titanium nickelide at nonuniform heating,” *Izv. Ross. Akad. Nauk. Ser. Phys.* **81** (11), 1451–1457 (2017).
6. E. V. Chernyaeva, V. A. Andreev, and Yu. N. V'yunenko, “Radial distribution of physical properties in a titanium-nickelide rod after a warm forging,” *Vestn. Tambov Univer., Ser. Estestv. Tekhn. Nauki* **23** (122), 310–312 (2018).
7. V. A. Andreev, V. S. Yusupov, M. M. Perkas, and N. V. Yakushevich, “Hot rotational forging of rods 2–20 mm in diameter fabricated of titanium-nickelide-based shape memory alloys,” in *Advanced Materials and Technologies*, Ed. by V. V. Klubovich (VGTV, Vitebsk, 2017), Vol. 1, pp. 61–69.
8. V. A. Andreev, V. S. Yusupov, M. M. Perkas, V. V. Prosvirnin, A. E. Shelest, S. D. Prokoshkin, I. Yu. Khmelevskaya, A. V. Korotitskii, S. A. Bondareva, and P. D. Karelin, “Mechanical and functional properties of commercial semifinished products of the TN-1 alloy manufactured by warm rotational forging and ECAP,” *Deform. Razrushenie Mater*, No. 4, 43–48 (2017).
9. A. M. Glezer, R. V. Sundeev, L. S. Metlov, A. A. Tomchuk, and L. F. Muradimova, “Megaplastic deformation: two main principles and seven specific features,” in *Proceedings of XXIII Petersburg Readings on the Strength Problems* (VVM, St. Petersburg, 2018), p. 191.
10. N. N. Belousov, V. N. Varyukhin, Yu. N. V'yunenko, and E. V. Chernyaeva; “Initiation and in situ study of the structure–phase changes in metastable alloys at torsion under pressure,” in *Proceedings of 60th International Scientific Conference Topical Problems of Strength* (VGTV Vitebsk, 2018), pp. 328–330.
11. A. M. Glezer and L. S. Metlov, “Megaplastic deformation of solids,” *Fiz. Tekhn. Vys. Davl.* **8** (4), 21–35 (2008).
12. R. V. Sundeev, A. V. Shalimova, and A. M. Glezer, “Bridgman-anvil deformation of titanium-, iron-, and zirconium-nickelide-based metallic alloys,” in *Pro-*

- ceedings of XXI Petersburg Readings on the Strength Problems* (Solo, St. Petersburg, 2014), pp. 288–292.
13. E. D. Merson, M. L. Linderov, I. N. Pigaleva, and E. D. Khafizova, “Effect of equal-channel angular pressing on the acoustic emission behavior and the fatigue fracture mechanism of the AL4-1 alloy,” *Vektor Nauki TGU*, No. 3, 223–226 (2013).
 14. V. V. Nosov, *Diagnostics of Machinery and Equipment: Textbook* (Lan’, St. Petersburg, 2012).
 15. A. S. Mahmud, H. Yang, S. Tee, G. Rio, and Y. Liu, “Effect of annealing on deformation-induced martensite stabilization of NiTi,” *Inermetallics* **16** (2), 209–214 (2008).
 16. N. N. Resnina, S. P. Belyaev, A. V. Sibirev, V. V. Rubanik, V. V. Rubanik Jr., and A. V. Lesota, “Effect of martensite stabilization in a TiNi alloy,” in *Proceedings of XXIII Petersburg Readings on the Strength Problems* (VVM, St. Petersburg, 2018), p. 139.
 17. I. Yu. Khmelevskaya, P. D. Karelin, S. D. Prokoshkin, V. A. Andreev, V. S. Yusupov, M. M. Perkas, V. V. Prosvirnin, A. E. Shelest, and V. S. Komarov, “Effect of the quasi-continuous equal-channel angular pressing on the structure and functional properties of Ti–Ni-based shape memory alloys,” *Phys. Met. Metallogr.* **118** (3), 279–287 (2017).

Translated by Yu. Ryzhkov